

# Infrared photodissociation spectra and solvation structures of $\text{Mg}^+(\text{CH}_3\text{OH})_n$ ( $n = 1-4$ )

Hironobu Machinaga<sup>a</sup>, Kazuhiko Ohashi<sup>b,\*</sup>, Yoshiya Inokuchi<sup>c</sup>,  
Nobuyuki Nishi<sup>c</sup>, Hiroshi Sekiya<sup>b</sup>

<sup>a</sup> *Department of Molecular Chemistry, Graduate School of Sciences, Kyushu University,  
Hakozaki, Fukuoka 812-8581, Japan*

<sup>b</sup> *Department of Chemistry, Faculty of Sciences, Kyushu University,  
Hakozaki, Fukuoka 812-8581, Japan*

<sup>c</sup> *Institute for Molecular Science, Myodaiji, Okazaki 444-8585, Japan*

## Abstract

The infrared photodissociation spectra of mass-selected  $\text{Mg}^+(\text{CH}_3\text{OH})_n$  ( $n = 1-4$ ) are measured and analyzed with the aid of density functional theory calculations. Hydrogen bonding between methanol molecules is found to be absent in  $\text{Mg}^+(\text{CH}_3\text{OH})_3$ , but detected in  $\text{Mg}^+(\text{CH}_3\text{OH})_4$  through characteristic frequency shifts of the OH stretch of methanol. The maximum number of the methanol molecules that can be directly bonded to the  $\text{Mg}^+$  ion is limited to three and the fourth molecule starts to fill the second solvation shell. The vibrational spectroscopy provides clear evidence for the closure of the first shell at  $n = 3$ .

---

\* Corresponding author. Fax: +81-92-642-2607.

*E-mail address:* kazu.scc@mbox.nc.kyushu-u.ac.jp (K. Ohashi).

## 1. Introduction

The process of ion solvation has been studied extensively for a wide variety of ions and solvents [1]. High-pressure mass spectrometry has been used to obtain enthalpies and free energies of association as a function of solvent number [2,3], providing insight into the presence of solvent shells. Time-of-flight mass spectrometry [4] and flow-tube studies [3] have also found great utility in identifying solvated ions of unusual stability through the observation of magic numbers. More detailed information on the ion solvation has become available through spectroscopic studies of the solvated ions. Vibrational spectroscopy of singly-charged alkali metal ions solvated by H<sub>2</sub>O and CH<sub>3</sub>OH has provided evidence for the formation of the second solvation shell before the complete filling of the first shell [5]. Electronic spectroscopy has been applied to singly-charged alkaline earth metals solvated by polar molecules, since the electronic transitions of the single valence electron offer a convenient probe of the local solvation environment around the metal ion [6,7].

The Mg<sup>+</sup>(CH<sub>3</sub>OH)<sub>n</sub> system has been the subject of previous investigations. Bauschlicher and co-workers carried out extensive theoretical calculations to predict geometrical structures and binding energies for  $n = 1$  and 2 as well as vertical transition energies for  $n = 1$  [8–10]. In flow-tube reactions studied by Castleman and co-workers, successive solvation products were observed without H-atom elimination up to  $n = 6$  [11]. Stace and co-workers examined the gas-phase chemistry of Mg<sup>+</sup> and Mg<sup>2+</sup> in association with methanol clusters and found that the Mg<sup>+</sup>(CH<sub>3</sub>OH)<sub>n</sub> ions show “product switching” via H-atom elimination when  $n \geq 3$  [12]. Lu and Yang performed mass spectrometric experiments with supporting *ab initio* calculations to facilitate the interpretation of the product switching behavior [13]. Stepwise binding energies were determined in collision-induced dissociation experiments with supporting *ab initio* calculations by Armentrout and co-workers [14]. Photodissociation spectrum of Mg<sup>+</sup>(CH<sub>3</sub>OH)<sub>1</sub> in the ultraviolet (UV) region was reported by Duncan and co-workers [15]. More recently, Farrar and co-workers carried out UV/visible photodissociation spectroscopy of Mg<sup>+</sup>(CH<sub>3</sub>OD)<sub>n</sub> ( $n = 1-5$ ) [16]. The spectra exhibit substantial red shifts as the second and third methanol

molecules are added, but the addition of the fourth or fifth molecule results in small red shift. The observation was interpreted in terms of the closure of the first solvent shell with three methanol molecules.

In this work, we apply vibrational spectroscopy to  $\text{Mg}^+(\text{CH}_3\text{OH})_n$  ( $n = 1-4$ ). The method has capability of probing the solvation structures more directly, since the OH stretch of methanol is extremely sensitive to changes in its bonding environment. Density functional theory (DFT) calculations are also performed to obtain minimum-energy structures and corresponding infrared (IR) spectra of  $\text{Mg}^+(\text{CH}_3\text{OH})_n$ . The comparison of the experimental and theoretical results provides information on the size of the first solvent shell.

## 2. Experimental and computational

The IR photodissociation spectra of  $\text{Mg}^+(\text{CH}_3\text{OH})_n$  ( $n = 1-4$ ) are measured by using a triple quadrupole mass spectrometer [17]. The solvated metal ions are produced in a laser vaporization source. The parent ions of interest are isolated by the first quadrupole mass filter. After deflection by an ion bender, the ions are introduced into the second quadrupole ion guide and irradiated by an infrared laser (Continuum, Mirage 3000). The vibrational excitation induces fragmentation of the parent ions. After leaving the ion guide, the fragment ions are analyzed by the third quadrupole mass spectrometer. The spectra are taken by recording the yields of the fragment ions as a function of wavenumber of the infrared laser.

The  $(\text{CH}_3\text{OH})_{n-1}\text{Mg}^+-\text{CH}_3\text{OH}$  bond dissociation energies were measured by Armentrout and co-workers [14]:  $1.51 \pm 0.07$ ,  $1.25 \pm 0.07$ , and  $0.95 \pm 0.09$  eV for  $n = 1-3$ , respectively. The observation of photodissociation in the  $3000-3800 \text{ cm}^{-1}$  ( $0.37-0.47$  eV) region indicates either that the  $\text{Mg}^+(\text{CH}_3\text{OH})_n$  ions have substantial amount of internal energies or that the ions absorb multiple photons. We believe that one-photon processes contribute predominantly to the spectra, since the infrared laser is unfocused in the present experiment. It follows that we detect only a hot subset of the clusters with internal energies sufficient for one-photon dissociation. As a result, the spectra of smaller clusters are quite noisy because of low photodissociation yield and the spectral features are fairly broad due to

overlapping hot bands. “Rare-gas tagging” method is often employed to remedy such a situation [18–21], where an argon atom is attached to clusters. The method produces efficient fragmentation thanks to small dissociation energy and decreases bandwidths without introducing significant spectral shifts. We therefore measure the spectra of  $\text{Mg}^+(\text{CH}_3\text{OH})_n\text{-Ar}$  when necessary.

Theoretical calculations are carried out with GAUSSIAN 98 program package [22] using the hybrid DFT method (B3LYP) with 6-31+G\* basis sets. The geometries of  $\text{Mg}^+(\text{CH}_3\text{OH})_n$  ( $n = 1\text{--}4$ ) are optimized without any symmetry constraints. We do not intend to carry out comprehensive calculations to locate all the possible isomers at high levels of theory. The main purpose is to predict theoretical IR spectra of  $\text{Mg}^+(\text{CH}_3\text{OH})_n$ . The harmonic vibrational frequencies and IR absorption intensities are evaluated for comparing the theoretical IR spectra with the observed ones. The frequencies of all the vibrations of all the species are scaled with a factor of 0.9782, which is chosen to reproduce the OH stretching frequency of the gas-phase methanol molecule ( $3681\text{ cm}^{-1}$ ).

### 3. Results and discussion

#### 3.1. Minimum-energy structures

Geometries of  $\text{Mg}^+(\text{CH}_3\text{OH})_n$  have been optimized for  $n = 1$  and 2 at the SCF/TZ2P level by Bauschlicher and co-workers [8–10], for  $n = 1\text{--}5$  at the UHF/6-31G\* level by Lu and Yang [13], and for  $n = 1\text{--}3$  at the MP2/6-31G\* level by Armentrout and co-workers [14]. The stable structures obtained from our calculations are consistent with those from the previous calculations, except as noted. We only briefly describe the qualitative aspects of our results as well as the previous ones [8–14].

The  $\text{Mg}^+$  ion is bonded to the oxygen atom of methanol in  $\text{Mg}^+(\text{CH}_3\text{OH})_1$  (see structure 1 in Fig.10 of ref. [13]). The 3s valence electron on  $\text{Mg}^+$  is not involved in bonding, but polarized away from methanol by mixing in some 3p character. The structure of methanol changes little from the free molecule, indicating the electrostatic nature of the bond between  $\text{Mg}^+$  and methanol.  $\text{Mg}^+(\text{CH}_3\text{OH})_2$  adopts bent structures, where two methanol

molecules are located on the same side of  $\text{Mg}^+$  to avoid the high density of the valence electron localized on the other side. Two bent geometries (with  $C_1$  and  $C_2$  symmetry) have been found for  $\text{Mg}^+(\text{CH}_3\text{OH})_2$  (structures **2a** and **2b** in Fig.10 of ref. [13]), which result from different orientation of the two OH groups. The relative stability of the two geometries interchanges depending on the levels of theory. From our calculations, the  $C_2$  structure is more stable, as reported by Armentrout and co-workers [14].

Fig. 1a exhibits stable structures of  $\text{Mg}^+(\text{CH}_3\text{OH})_3$ . In structure 3I, all the three methanol molecules are directly bonded to  $\text{Mg}^+$ . The third methanol is located on the same side of  $\text{Mg}^+$  as the first two molecules, again avoiding the polarized valence electron. In structure 3II, on the other hand, only two methanol molecules are directly bonded to  $\text{Mg}^+$ , forming the first solvation shell, and the third molecule is bonded to the two methanol molecules in the first shell through two hydrogen bonds. Lu and Yang found that structure 3I is more stable than structure 3II [13].

Three structures are examined for  $\text{Mg}^+(\text{CH}_3\text{OH})_4$ , which are illustrated in Fig. 1b. Both structures 4I and 4II have only three methanol molecules in the first shell. The fourth molecule is bonded to the two methanol molecules in the first shell through two hydrogen bonds in structure 4I, whereas it interacts with only one methanol molecule through a hydrogen bond in structure 4II. In structure 4III, four methanols are directly bonded to  $\text{Mg}^+$ , forming the first shell. Similar to the smaller clusters, all methanol molecules prefer to reside on the same side of  $\text{Mg}^+$ , avoiding the valence electron. Lu and Yang showed that structure 4III is less stable than structures 4I and 4II [13], obviously due to large repulsion among methanol molecules in the first shell.

### 3.2. Photodissociation spectra

The  $\text{Mg}^+(\text{CH}_3\text{OH})_n$  ions are the dominant species until  $n = 4$ . The switching from  $\text{Mg}^+(\text{CH}_3\text{OH})_n$  to H-atom elimination product occurs at  $n = 5$ , as reported by Lu and Yang [13]. As a result, the intensity of  $\text{Mg}^+(\text{CH}_3\text{OH})_n$  produced in our laser vaporization source is significantly small for  $n \geq 5$ , precluding the measurement of the photodissociation spectra.

Fig. 2 displays the IR photodissociation spectra of  $\text{Mg}^+(\text{CH}_3\text{OH})_n$  ( $n = 1-4$ ) in the 3000–3800  $\text{cm}^{-1}$  region. These spectra are recorded by monitoring the  $\text{Mg}^+(\text{CH}_3\text{OH})_{n-1}$  fragment ions. A prominent band is observed around 3520, 3590, and 3590  $\text{cm}^{-1}$  in each of the spectra for  $n = 1-3$ , respectively. We assign these bands to the free OH stretch of methanol. No appreciable absorption is seen below 3500  $\text{cm}^{-1}$  for  $n = 2$  and 3, suggesting the absence of hydrogen bonding between methanol molecules. The addition of the fourth methanol molecule drastically affects the spectrum, yielding broad features with significant intensity in the 3000–3500  $\text{cm}^{-1}$  region. The appearance of new maxima around 3225 and 3355  $\text{cm}^{-1}$  is suggestive of hydrogen bonding between methanol molecules. The position of the highest-frequency band (3600  $\text{cm}^{-1}$ ) is similar to the free OH stretch in  $\text{Mg}^+(\text{CH}_3\text{OH})_2$  and  $\text{Mg}^+(\text{CH}_3\text{OH})_3$ , indicating that at least one methanol in  $\text{Mg}^+(\text{CH}_3\text{OH})_4$  does not act as an H-atom donor.

### 3.3. $\text{Mg}^+(\text{CH}_3\text{OH})_1$ and $\text{Mg}^+(\text{CH}_3\text{OH})_2$

The spectrum of  $\text{Mg}^+(\text{CH}_3\text{OH})_1$  (Fig. 2a) shows a broad maximum around 3520  $\text{cm}^{-1}$  with a shoulder around 3600  $\text{cm}^{-1}$ . In the spectrum measured via the argon tagging (not shown), these features collapse into sharp bands peaked at 3560 and 3612  $\text{cm}^{-1}$ . It should be noted that the apparent blue shift of the maximum from 3520 to 3560  $\text{cm}^{-1}$  upon the argon tagging does not necessarily imply an increase in the frequency of the OH stretch. This is because we detect only a hot subset of the clusters with large internal energies in the measurement without argon tagging; the transitions observed in the spectrum of  $\text{Mg}^+(\text{CH}_3\text{OH})_n$  are not the solo OH stretch fundamental but the transitions involving sequences of vibrations. We ascribe the shift to frequency reductions of these vibrations in the upper levels. The strong 3560  $\text{cm}^{-1}$  band is assigned to the free OH stretch of the methanol molecule. The weak 3612  $\text{cm}^{-1}$  band is tentatively attributed to a combination band involving an intermolecular vibration. The position of the OH stretch is red-shifted 121  $\text{cm}^{-1}$  from that of the gas-phase methanol. For  $\text{Mg}^+(\text{CH}_3\text{OH})_2$ , the absorption maximum is seen around 3590  $\text{cm}^{-1}$  (Fig. 2b) and the corresponding band in the argon tagging

spectrum (not shown) is located at  $3600\text{ cm}^{-1}$ , resulting in a smaller shift of  $81\text{ cm}^{-1}$  relative to the gas-phase methanol. The decreasing red shift with increasing solvent number indicates that the interaction between  $\text{Mg}^+$  and methanol in  $\text{Mg}^+(\text{CH}_3\text{OH})_2$  is weaker than that in  $\text{Mg}^+(\text{CH}_3\text{OH})_1$ , which is consistent with the result that the second methanol is bound less strongly than the first one [14].

### 3.4. $\text{Mg}^+(\text{CH}_3\text{OH})_3$

In Fig. 3, the experimental spectrum of  $\text{Mg}^+(\text{CH}_3\text{OH})_3$  is compared with the theoretical spectra of isomers 3I and 3II. The theoretical spectrum of 3I (Fig. 3b) displays nearly degenerate free OH stretches of the three methanol molecules in first shell at  $3630$ ,  $3632$ , and  $3633\text{ cm}^{-1}$ . In the spectrum of 3II (Fig. 3c), on the other hand, hydrogen-bonded OH stretches are located at  $3368$  and  $3416\text{ cm}^{-1}$  in addition to the free OH stretch of the methanol molecule in the second shell at  $3655\text{ cm}^{-1}$ . The experimental spectrum exhibits no appreciable absorption in the region of the hydrogen-bonded OH stretches, indicating that isomer 3II is absent under the present experimental conditions. The position of the  $3590\text{ cm}^{-1}$  band is in agreement with those of the free OH stretches of isomer 3I. Thus the IR spectroscopy verifies that the most stable structure of  $\text{Mg}^+(\text{CH}_3\text{OH})_3$  is isomer 3I, in which all the three methanol molecules are directly bonded to  $\text{Mg}^+$ .

### 3.5. $\text{Mg}^+(\text{CH}_3\text{OH})_4$

Fig. 4 compares the experimental spectrum of  $\text{Mg}^+(\text{CH}_3\text{OH})_4$  with the theoretical spectra of isomers 4I–4III. Hydrogen-bonded OH stretches are located at  $3405$  and  $3447\text{ cm}^{-1}$  in the theoretical spectrum of 4I (Fig. 4b). On the other hand, the spectrum of 4II (Fig. 4c) displays a hydrogen-bonded OH stretch at  $3198\text{ cm}^{-1}$ . The other transitions located above  $3600\text{ cm}^{-1}$  are due to the free OH stretches. Two of the four OH stretches of isomer 4III ( $3554$  and  $3572\text{ cm}^{-1}$ ) are red-shifted  $55$ – $73\text{ cm}^{-1}$  relative to the others ( $3626$  and  $3627\text{ cm}^{-1}$ ), which can be regarded as characteristic bands of this isomer (Fig. 4d).

Two maxima observed around  $3400$  and  $3250\text{ cm}^{-1}$  in Fig. 4a seem to be due to

hydrogen-bonded OH stretches of isomers 4I and 4II, respectively. The experimental spectrum can be reproduced by a superposition of the theoretical spectra for 4I and 4II, suggesting the coexistence of both isomers. However, it is hard to ascertain the presence of isomer 4III, because the high-energy tail of the hydrogen-bonded OH stretches extends to the position of the free OH stretches characteristic of isomer 4III. Therefore we use the argon tagging technique to collapse the broad features. One may suspect that the argon tagging affects the position and intensity of the OH stretches. Our DFT calculations indicate that the attachment of argon to the OH group of methanol shifts the position of the OH stretch by  $\approx 35$   $\text{cm}^{-1}$  and enhances the intensity by a factor of  $\approx 2$ . Since the spectral changes are small compared to large difference in the spectral features among isomers 4I–4III, we can safely compare the experimental spectrum of  $\text{Mg}^+(\text{CH}_3\text{OH})_4\text{-Ar}$  with the theoretical spectra of  $\text{Mg}^+(\text{CH}_3\text{OH})_4$  to discriminate the isomeric structures.

Fig. 4e represents the spectrum of  $\text{Mg}^+(\text{CH}_3\text{OH})_4\text{-Ar}$  measured by monitoring the Ar loss channel. The continuous background seen in Fig. 4a is suppressed and the strong feature around  $3250$   $\text{cm}^{-1}$  disappears completely. The two bands peaked at  $3330$  and  $3380$   $\text{cm}^{-1}$  are assignable to the hydrogen-bonded OH stretches of isomers 4I. The  $3430$  and  $3490$   $\text{cm}^{-1}$  bands are tentatively attributed to combination bands. Actually, our DFT calculations predict 11 vibrational modes with frequencies below  $120$   $\text{cm}^{-1}$  including intermolecular vibrations and internal rotations of the methyl groups, several of which give rise to possible combination bands. The coexistence of isomer 4III is unlikely, because no absorption is recognized in the  $3520\text{--}3600$   $\text{cm}^{-1}$  region, where the free OH stretches characteristic of isomer 4III are expected. The argon tagging method provides a cold subset of the clusters in an otherwise warm distribution [19]. Thus the IR spectroscopy with the argon tagging technique proves that isomer 4I is the most stable form of  $\text{Mg}^+(\text{CH}_3\text{OH})_4$ , in which the number of the methanol molecules that can be directly bonded to  $\text{Mg}^+$  is limited to three.

### 3.6. Solvation structures

Farrar and co-workers reported the photodissociation spectra of  $\text{Mg}^+(\text{CH}_3\text{OD})_n$  ( $n = 1\text{--}5$ ) in the  $15000\text{--}45000$   $\text{cm}^{-1}$  region [16]. The electronic transitions observed in these clusters are based on the excitation of the  $^2\text{P}\text{--}^2\text{S}$  transitions of  $\text{Mg}^+$ . The higher-energy band

of  $n = 2$  exhibits a large red shift upon the addition of the third methanol molecule. In the spectra of  $n = 4$  and 5, however, the band shows no red shift relative to  $n = 3$ . They interpreted these spectral features in terms of the closure of the first solvation shell at  $n = 3$ , as observed in the  $\text{Mg}^+(\text{H}_2\text{O})_n$  system by Fuke and co-workers [23].

The present study demonstrates that the IR spectroscopy enables us to investigate the solvation structures of  $\text{Mg}^+(\text{CH}_3\text{OH})_n$  more directly by probing hydrogen-bonding interactions among solvent molecules through the OH stretch of methanol. The  $n = 3$  spectrum reveals that all the three methanol molecules are directly bonded to  $\text{Mg}^+$  to form the first solvation shell. The  $n = 4$  spectrum detects the formation of hydrogen bonds between methanol molecules; the fourth molecule prefers to bind to methanols in the first shell rather than squeeze into the first shell. Thus, the IR spectroscopy clearly shows that the first solvation shell of  $\text{Mg}^+(\text{CH}_3\text{OH})_n$  is completed with three methanol molecules, and the fourth molecule starts to fill the second shell. These observations are totally consistent with the results of the electronic spectroscopy [16] and also with the lowest-energy structures obtained from theoretical calculations [13].

The solvation structures of  $\text{Mg}^+(\text{CH}_3\text{OH})_n$  share many features with the  $\text{Mg}^+(\text{H}_2\text{O})_n$  system [23,24]. However, the closure of the first shell with three solvent molecules is not inherent in the  $\text{Mg}^+$  ion, because the electronic spectroscopy with supporting *ab initio* calculations suggested that four ammonia molecules are directly bonded to  $\text{Mg}^+$  in the most stable forms of  $\text{Mg}^+(\text{NH}_3)_4$  [7,25]; the suggestion has recently been confirmed by our group through the IR spectroscopy [26]. The competition between the ion–solvent and solvent–solvent interactions probably determines the overall solvation structures. The water and methanol molecules have a propensity to engage in highly networked or chained hydrogen-bonding interactions. The strong solvent–solvent interactions play a role in forming the solvation structures observed in the  $\text{Mg}^+(\text{H}_2\text{O})_n$  and  $\text{Mg}^+(\text{CH}_3\text{OH})_n$  systems.

### Acknowledgement

We thank Dr. K. Ohshimo for his help in equipping our photodissociation

spectrometer with the laser vaporization source. This work was supported in part by the Joint Studies Program (2003) of the Institute for Molecular Science.

## References

- [1] A. W. Castleman, Jr., K. H. Bowen, *J. Phys. Chem.* 100 (1996) 12911.
- [2] P. Kebarle, *Ann. Rev. Phys. Chem.* 28 (1977) 445.
- [3] A. W. Castleman, Jr., R. G. Keesee, *Chem. Rev.* 86 (1986) 589.
- [4] T. D. Märk, *Int. J. Mass Spectrom. Ion Processes* 79 (1987) 1.
- [5] J. M. Lisy, *Int. Rev. Phys. Chem.* 16 (1997) 267.
- [6] K. Fuke, K. Hashimoto, S. Iwata, *Adv. Chem. Phys.* 110 (1999) 431.
- [7] J. M. Farrar, *Int. Rev. Phys. Chem.* 22 (2003) 593.
- [8] C. W. Bauschlicher, Jr., H. Partridge, *J. Phys. Chem.* 95 (1991) 3946.
- [9] C. W. Bauschlicher, Jr., H. Partridge, *J. Phys. Chem.* 95 (1991) 9694.
- [10] M. Sodupe, C. W. Bauschlicher, Jr., *Chem. Phys. Lett.* 195 (1992) 494.
- [11] A. C. Harms, S. N. Khanna, B. Chen, A. W. Castleman, Jr., *J. Chem. Phys.* 100 (1994) 3540.
- [12] C. A. Woodward, M. P. Dobson, A. J. Stace, *J. Phys. Chem. A* 101 (1997) 2279.
- [13] W. Lu, S. Yang, *J. Phys. Chem. A* 102 (1998) 825.
- [14] A. Andersen, F. Muntean, D. Walter, C. Rue, P. B. Armentrout, *J. Phys. Chem. A* 104 (2000) 692.
- [15] M. R. France, S. H. Pullins, M. A. Duncan, *Chem. Phys.* 239 (1998) 447.
- [16] J. I. Lee, D. C. Sperry, J. M. Farrar, *J. Chem. Phys.* 114 (2001) 6180.
- [17] Y. Inokuchi, N. Nishi, *J. Chem. Phys.* 114 (2001) 7059.
- [18] M. B. Knickelbein, W. J. C. Menezes, *Phys. Rev. Lett.* 69 (1992) 1046.
- [19] P. Ayotte, G. H. Weddle, J. Kim, M. A. Johnson, *Chem. Phys.* 239 (1998) 485.
- [20] N. L. Pivonca, C. Kaposta, M. Brümmer, G. von Helden, G. Meijer, L. Wöste, D. M. Neumark, K. R. Asmis, *J. Chem. Phys.* 118 (2003) 5275.
- [21] G. Gregoire, N. R. Brinkmann, D. van Heijnsbergen, H. F. Schaefer, M. A. Duncan, *J. Phys. Chem. A* 101 (1997) 2279.
- [22] M. J. Frisch et al., Gaussian, Inc., Pittsburgh PA, 1998.

- [23] F. Misaizu, M. Sanekata, K. Fuke, S. Iwata, J. Chem. Phys. 100 (1994) 1161.
- [24] Y. Inokuchi, K. Ohshimo, F. Misaizu, N. Nishi, submitted to J. Phys. Chem. A.
- [25] S. Yoshida, K. Daigoku, N. Okai, A. Takahata, A. Sabu, K. Hashimoto, K. Fuke, J. Chem. Phys. 117 (2002) 8657.
- [26] K. Ohashi et al., in preparation.

Review Copy

**Figure captions**

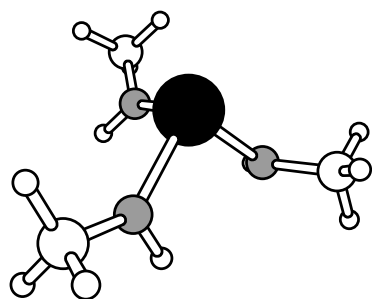
Fig. 1. Structures of  $\text{Mg}^+(\text{CH}_3\text{OH})_n$  with (a)  $n = 3$  and (b)  $n = 4$  obtained from DFT calculations at the B3LYP/6-31+G\* level. Magnesium and oxygen atoms are denoted by solid and shaded circles, respectively.

Fig. 2. IR photodissociation spectra of  $\text{Mg}^+(\text{CH}_3\text{OH})_n$  ( $n = 1-4$ ) in the 3000–3800  $\text{cm}^{-1}$  region. Amplitude of four spectra is normalized independently at each maximum.

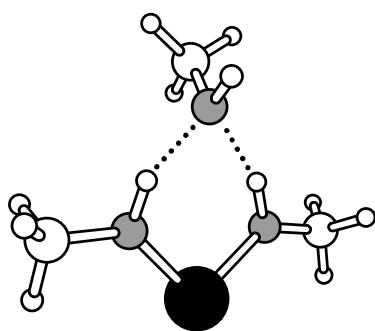
Fig. 3. (a) Experimental spectrum of  $\text{Mg}^+(\text{CH}_3\text{OH})_3$  reproduced from Fig. 2c. Theoretical spectra obtained from DFT calculations for structures (b) 3I and (c) 3II. Intensity of the spectrum of 3I is magnified by a factor of 10 for clear comparison.

Fig. 4. Experimental spectra of (a)  $\text{Mg}^+(\text{CH}_3\text{OH})_4$  reproduced from Fig. 2d and (e)  $\text{Mg}^+(\text{CH}_3\text{OH})_4\text{-Ar}$ . Theoretical spectra obtained from DFT calculations for structures (b) 4I, (c) 4II, and (d) 4III. Intensity of the spectrum of 4III is magnified by a factor of 5.

(a)

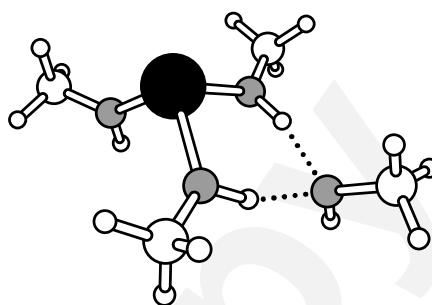


3I

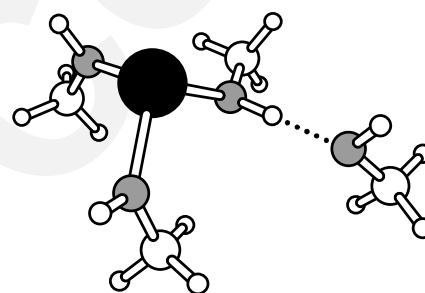


3II

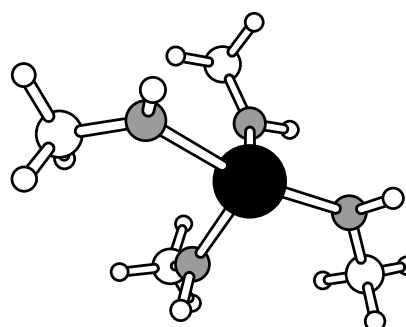
(b)



4I



4II



4III

Fig.1 Machinaga *et al.*

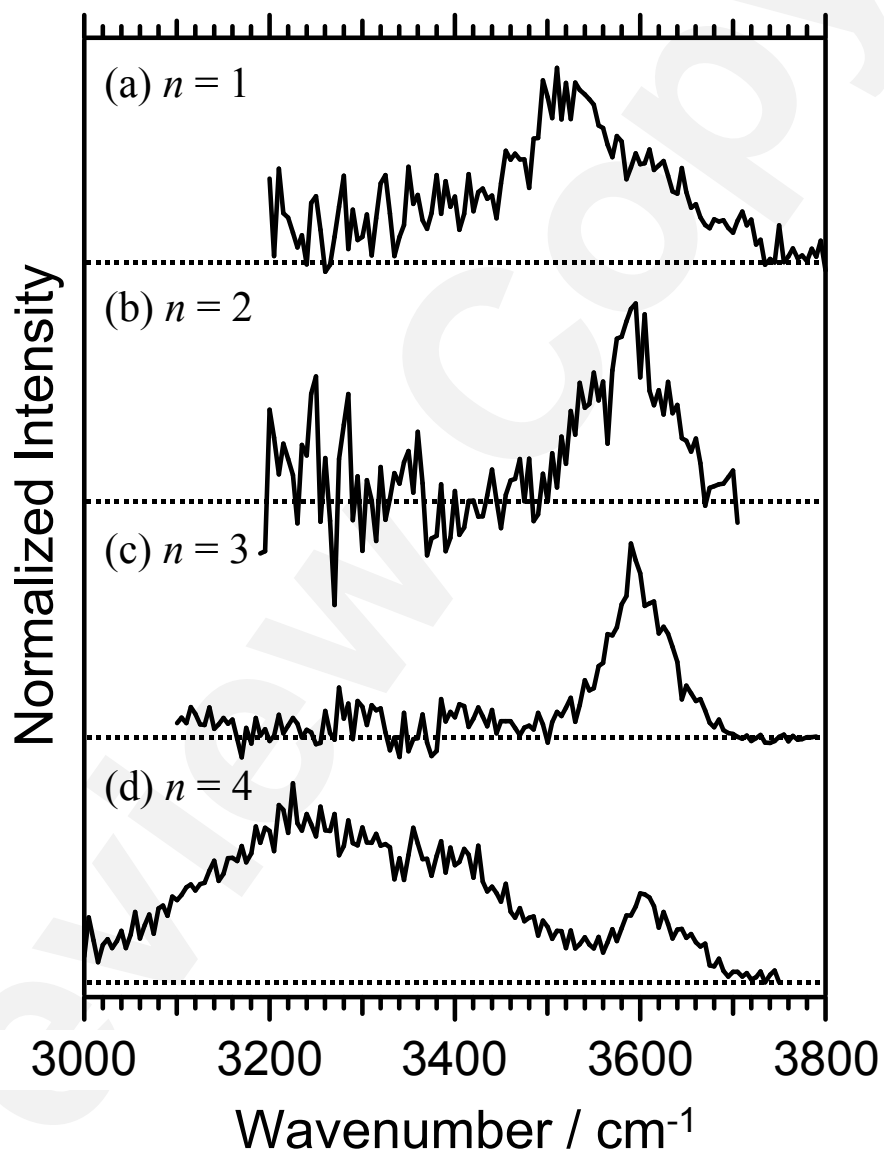


Fig.2 Machinaga *et al.*

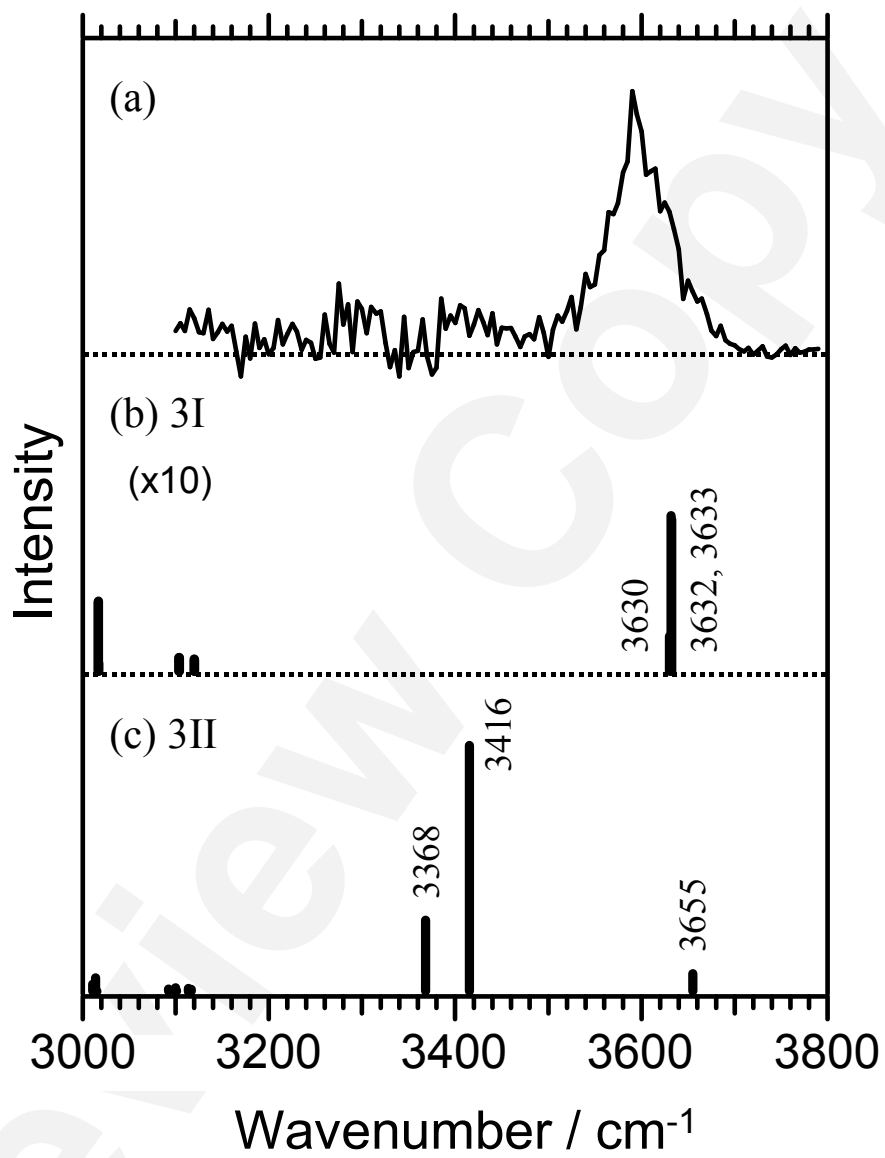


Fig.3 Machinaga *et al.*

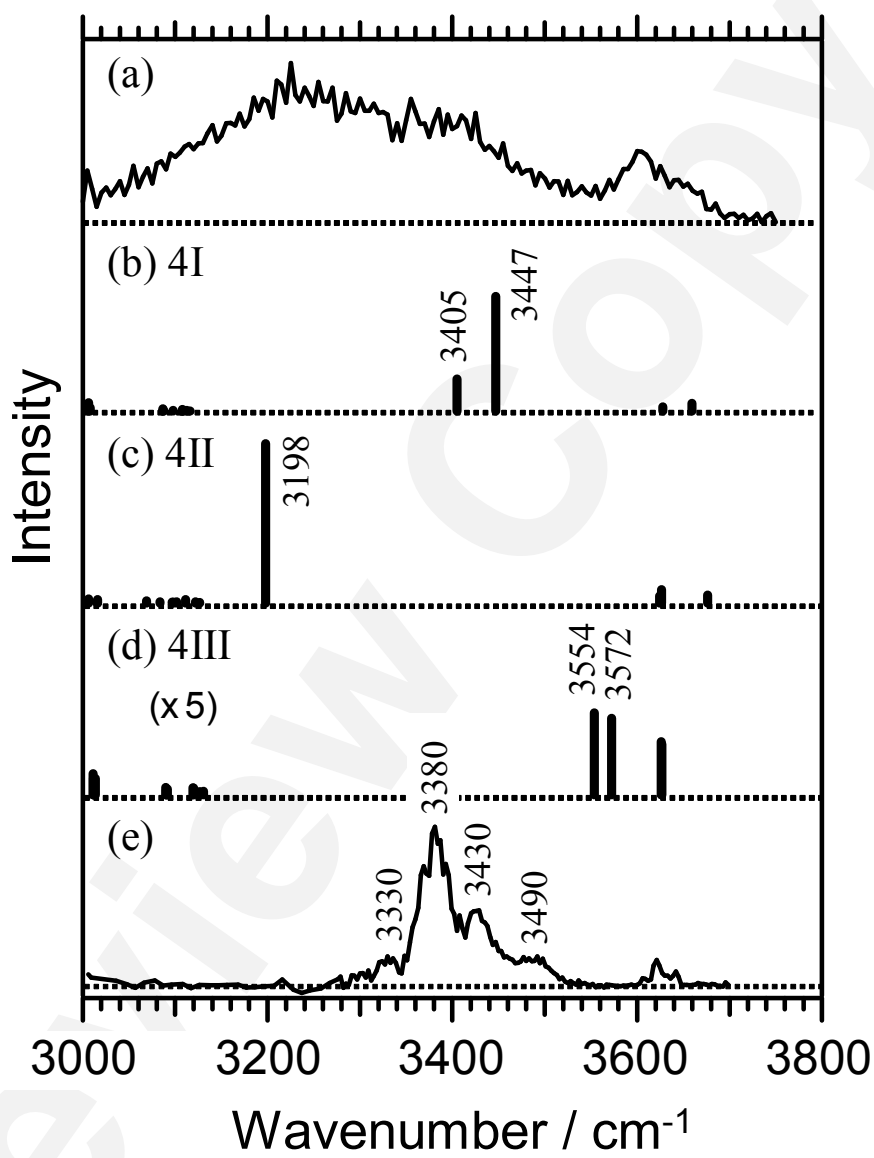


Fig.4 Machinaga *et al.*